Curvature tensor of a statistical manifold associated with a correlated-walk model

Tsunehiro Obata
Department of Electrical Engineering, Gunma National College of Technology, 580 Toriba-machi, Maebashi 371, Japan

Hiroshi Oshima
Department of Physics, Toho University School of Medicine, 5-21-16 Ohmori-nishi, Ota-ku, Tokyo 143, Japan

Hiroaki Hara
Graduate School of Information Science, Tohoku University, Aoba-ku, Sendai 980, Japan
(Received 25 November 1996)

The curvature tensor of a statistical manifold associated with a correlated-walk model is investigated. In the model, a walker moves along a linear lattice right or left or stays, depending on the last steps. In the case of symmetric walks, two jump probabilities and a stay probability (r_0) specify the transition probabilities and constitute a three-dimensional (3D) space. The 3D space is foliated by the stay probability r_0. A Riemann curvature, defined by the method of information geometry, on each 2D leaf is not only a function of two jump parameters, but also a step time N. The dynamic evolution of the Riemann scalar curvature R and also the asymptotic properties of the R in $N\to\infty$ are investigated in detail. It is found that remarkable features appear in the dynamic process of the R. Such dynamic features of the R are able to be well understood in terms of the degree of correlation or the activity of stepping. In $N\to\infty$, each leaf is shown to approach the saddle surface of $R=-1$ except for the leaf of $r_0=1$. The exceptional leaf approaches the spherical surface of $R=\frac{1}{2}$. The values of R are shown to have relation to regularity of paths or stability of stochastic processes. The relation to stability is also discussed by contrast with the values of R of Fermi gases and Bose gases. It is shown that the R's of the leaves $r_0=0$ and 1 are almost equal to those of Fermi gases and Bose gases, respectively, and that the R's of the two leaves reflect the difference of the stability of the two leaves. The asymptotic property of a one-parameter curvature, called the a curvature, is also investigated. The a curvature at $a=1$ is shown to approach zero for $N\to\infty$ or approaching equilibrium states. This suggests that the zero $a=1$ curvature is a universal property in a broader class of equilibrium systems including thermodynamic systems. [S1063-651X(97)02707-4]

PACS number(s): 05.70.Ln, 05.40.+j, 02.40.−k, 02.50.−r

I. INTRODUCTION

A positive definite Riemann metric on thermodynamic state space was introduced by Ingarden *et al.* [1] and Ruppeiner [2]. With the metric tensor one can evaluate the Riemann curvature of thermodynamic state space. The thermodynamic Riemann curvature was first calculated for several cases by Ruppeiner [2,3]. The calculation led him to interpret the Riemann scalar curvature as a measure of effective interaction (see also Ref. [4]). On the other hand, Janyszek and Mrugala [5–7] interpreted it as a measure of stability on the basis of calculation of the scalar curvature for many thermodynamical models, including the models worked out by Ruppeiner.

Recently we tried to generalize the notion of the thermodynamic curvature as a measure of effective interaction or stability to nonequilibrium processes [8–10]. We introduced a metric tensor on a parameter space spanned by jump probabilities characterizing a stochastic process of random or correlated walks, using the receipt of information geometry. The metric tensor for stochastic processes, being different from equilibrium thermodynamic systems, develops in time. For instance, a D-dimensional random walk (RW) accompanies the expansion of a $2D$-dimensional sphere. As a step time N increases, the Riemann scalar curvature fades away as $1/N$. We regarded this decrease behavior of the curvature as a geometrical representation of approach from an initial unstable state to a stable equilibrium state [8]. This interpretation is consistent with the results for equilibrium systems: The curvature for stable equilibrium systems becomes small.

A walker of the RW model may move with step probabilities given at random, that is, without correlation between steps. In reality we find correlated motion almost everywhere. In successive papers [9,10], we examined the statistical manifold associated with a correlated-walk (CW) model. The space is spanned by two parameters representing the jump probabilities of the CW model. We there studied the Riemann scalar curvature R of the CW manifold, and showed that the time development of the CW manifold produces inhomogeneous expansion from a spherical surface of $R=\frac{1}{2}$ to a saddle surface of $R=-1$ through an era of violent oscillations. Such behavior of the Riemann scalar curvature was shown to be well understood in terms of ''stability'' and ''order parameter'' of stochastic processes. In other words, the calculation suggested that the interpretation of the Riemann scalar curvature as a measure of stability might be useful in the spaces of jump probabilities as well as in thermodynamic state space.

In the present paper we take a more complicated model of correlated walks, with an eye to investigating the space of jump probabilities characterizing the model. In the model, a walker moves along a linear lattice of infinite extension right

or left, and sometimes stays. The probabilities of jump or stay are supposed to depend on the previous steps. Namely, two successive steps are correlated. For simplicity we consider the case of symmetric walking, in which the number of independent parameters specifying the transition probabilities of jump or stay is three. The stay probability is represented by r_0. Here $r_0=1$ means that the walker stays and stays again, and $r_0=0$ means that the walker stays and then moves. The three-dimensional (3D) parameter space is foliated by the stay parameter $0\leqslant r_0\leqslant 1$, and each leaf is 2D. We examine the time development of the Riemann scalar curvature of each leaf and also the asymptotic properties of the leaf.

A scenario of the Riemann scalar curvature R is as follows. The R of every leaf starts from a spherical surface of $R=\frac{1}{2}$. The homogeneous space immediately deforms to an inhomogeneous space and the R rapidly decreases for a short time. After that, the R turns to increasing and finally approaches $\frac{1}{2}$ for the leaf $r_0=1$ and -1 for the leaves $r_0\neq 1$. In the dynamic process of the R, we find remarkable features. The 2D space is characterized by three regions. A region has small values of the R, and the region separates the other two regions from each other like a valley. In one side of the valley, the R is almost homogeneous. As the step time goes by, the homogeneous region gradually extends, and becomes more and more homogeneous. The extending region then swallows the valley and also the other side. These dynamic features of the R are shown to be well understood in terms of the degree of correlation or the activity of stepping. Furthermore, the differences of the asymptotic values of R are shown to have relation to regularity of paths or stability of stochastic processes. We note that the paths of the walkers of $r_0\neq 1$ extend infinitely, while the paths of the walkers of $r_0=1$ extend finitely. Thus we say that the R associated with continuous paths is smaller than the R associated with discontinuous paths. Generally speaking, the more regular a path the smaller the R. As another viewpoint we note that the R's for the leaf $r_0=1$ and the leaf $r_0=0$ are very similar to the R's of Fermi gases and Bose gases, investigated by Janyszek and Mrugala [6]. They showed that the stability of the ideal quantum gases can be measured by means of the R. Actually we show that the difference of the R between the two leaves can be well understood in terms of stability.

We also investigate the asymptotic property of a one-parameter curvature, called the a curvature. The $a=1$ curvature is found to approach zero, regardless of r_0, in the limit of infinite time or approaching equilibrium states. We show also that the equilibrium distribution functions of the $r_0\neq 1$ leaves are members of the so-called exponential family but those of the leaf $r_0=1$ are not so. Meanwhile any thermodynamic system is noted to have zero $a=1$ curvature. Upon such a result, we suggest that the zero $a=1$ curvature might be a universal property in a broader class of equilibrium systems including thermodynamic systems.

This paper is organized as follows. In Sec. II we first recapitulate some main expressions in information geometry, and then we apply the expressions to thermodynamics and also stochastic processes such as random walks or correlated walks. Some results of Ruppeiner [2–4] and Janyszek and Mrugala [5–7], and also some recent results of ours [8–10] are reviewed, paying attention to statistical manifolds. In Sec. III we consider the process of a walker jumping or staying correlatively, and we introduce the statistical manifolds associated with the process. Then a method of numerical analysis of the R is described and the numerical solutions are given. The a curvature is analytically obtained. The details of the calculation are given in the Appendix. In the final section IV we derive the scenario above on the basis of the numerical solutions and the analytic solutions.

II. INFORMATION GEOMETRY, THERMODYNAMICS, AND STOCHASTIC PROCESSES

We first recapitulate some main expressions in information geometry necessary for us. After that, we briefly review some results of Ruppeiner [2–4], Janyszek and Mrugala [5–7], and also some recent results of ours [8–10].

A. Information geometry

Today information geometry [11] teaches us that a metric and a one-parameter connection, called the a connection, can be naturally introduced on a parametrized family $S=\{p(x,\theta)|\,\theta\in\Omega\}$ of probability density functions $\rho(x,\theta)$, where x is a random variable, θ is a parameter, and Ω is a parameter space. Modern differential geometry provides some elegant treatments of the space S. But these treatments are not fundamental for the purposes of our research, so we follow the traditional method representing tensors by coordinate components.

The metric tensor is defined by Fisher's information matrix

$$g_{ij}(\theta)=E[\partial_i\ell\,\partial_j\ell]=-E[\partial_i\partial_j\ell], \tag{1}$$

with $\ell(x,\theta)=\ln p(x,\theta)$, the parameter-differential operator $\partial_i=\partial/\partial\theta^i$, and the expectation operation $E[\cdot]$ with respect to the distribution $\rho(x,\theta)$. The last equality is due to the normalization condition of probability. The metric tensor gives an inner product for two vectors at a point.

The a connection is defined by

$$\Gamma_{ijk}(\theta)=E\left[\partial_i\ell\left(\partial_j\partial_k\ell+\frac{1-a}{2}\,\partial_j\ell\,\partial_k\ell\right)\right]. \tag{2}$$

The connection prescribes a way of transporting a vector at a point to a neighboring point. In the case of $a=0$, the connection reduces to the so-called Levi-Cività connection

$$\Gamma^{(0)}_{ijk}=\tfrac{1}{2}(\partial_k g_{ij}+\partial_j g_{ik}-\partial_i g_{jk}). \tag{3}$$

If necessary, we express a value of a through the superscript as written above.

It is often useful to decompose the a connection as follows:

$$\Gamma_{ijk}=\Gamma^{(0)}_{ijk}-\frac{a}{2}\,T_{ijk}, \tag{4}$$

with

$$T_{ijk}(\theta)=E[\partial_i\ell\,\partial_j\ell\,\partial_k\ell]=-E[\partial_i\partial_j\partial_k\ell]-E[(\partial\ell_i)(\partial_j\partial_k\ell)+(\partial\ell_j)(\partial_k\partial_i\ell)+(\partial\ell_k)(\partial_i\partial_j\ell)]. \tag{5}$$

This tensor is completely symmetric. The last equality is due to the normalization condition of probability.

When a vector at a point is turned around a loop by the transportation rule, the vector at the same point after the transportation does not in general coincide with the vector before the transportation. The discrepancy between the two vectors is measured by the a-curvature tensor

$$R^i_{jkl}=\partial_k\Gamma^i_{jl}-\partial_l\Gamma^i_{jk}+\Gamma^i_{mk}\Gamma^m_{jl}-\Gamma^i_{ml}\Gamma^m_{jk}. \tag{6}$$

We here use the Misner-Thorne-Wheeler convention for the curvature sign [12]. This sign convention is opposite to Ruppeiner's [4].

The covariant representation

$$R_{ijkl}=g_{im}R^m_{jkl}=\partial_k\Gamma_{ijl}-\partial_l\Gamma_{ijk}-(\Gamma_{mik}+aT_{mik})\Gamma^m_{jl}+(\Gamma_{mil}+aT_{mil})\Gamma^m_{jk} \tag{7}$$

is useful. Substitution of the decomposition (4) yields

$$R_{ijkl}=R^{(0)}_{ijkl}-\frac{a}{2}(\nabla^{(0)}_k T_{ijl}-\nabla^{(0)}_l T_{ijk})+\frac{a^2}{4}g^{mn}(T_{mik}T_{njl}-T_{mil}T_{njk}), \tag{8}$$

with the covariant derivative with respect to the Levi-Cività connection $\nabla^{(0)}_k$.

Linear combination of the components of the curvature tensor produces some scalars. In particular, the scalar

$$R=g^{jl}R^k_{jkl} \tag{9}$$

is important. In the case of $a=0$, this scalar is the so-called Riemann scalar curvature.

When the formalism is applied to the exponential family

$$S=\left\{p(x,\theta)\middle|p(x,\theta)=\exp\left[C(x)+\sum_{i=1}^{n}\theta^iF_i(x)-\psi(\theta)\right]\right\}, \tag{10}$$

we have the metric

$$g_{ij}=\frac{\partial^2\psi}{\partial\theta^i\partial\theta^j} \tag{11}$$

and the $a=1$ connection

$$\Gamma^{(1)}_{ijk}=0. \tag{12}$$

Hence the exponential family is zero $a=1$ curvature, that is, $R^{(1)}_{ijkl}=0$. However, the Riemann curvature $R^{(0)}_{ijkl}$ does not vanish in general. In particular, the 2D Riemann scalar curvature may be written as follows [5]:

$$R^{(0)}=\frac{-1}{2g^2}\begin{vmatrix}\psi_{,11} & \psi_{,12} & \psi_{,22}\\ \psi_{,111} & \psi_{,112} & \psi_{,122}\\ \psi_{,112} & \psi_{,122} & \psi_{,222}\end{vmatrix}. \tag{13}$$

The g is the determinant of the metric tensor.

B. Application to thermodynamics

A metric on thermodynamic state space can be obtained by applying information geometry to the grand canonical distribution function

$$\frac{1}{\Xi}\exp[-\beta H+aN](=\exp[-\beta H+aN-\ln\Xi]), \tag{14}$$

with the Hamiltonian H and the number of particles N. The distribution function with the parameters a and β constitutes an exponential family. In the thermodynamic limit, the grand partition function Ξ is expressed by means of a thermodynamic potential ϕ:

$$\frac{k_B}{V}\ln\Xi=S-\frac{1}{T}u+\frac{\mu}{T}\rho\equiv\phi, \tag{15}$$

which in turn is equal to P/T, where V, P, and T are the volume, pressure, and temperature of the system. s, u, and ρ are the entropy, internal energy, and number density of particles per volume. There exist also the relations $T=(k_B\beta)^{-1}$ and $\mu=a\beta^{-1}$, where μ is the chemical potential and k_B is the Boltzmann constant.

Therefore the thermodynamic potential ϕ yields the metric

$$g_{ij}=\frac{\partial^2\ln\Xi}{\partial F^i\partial F^j}=\frac{V}{K_B}\frac{\partial^2\phi}{\partial F^i\partial F^j}, \tag{16}$$

with the coordinate system $F=(1/T,-\mu/T)$. Note that the thermodynamic metric is different only by the volume factor from that used by Ruppeiner [4]. So our Riemann curvature tensor is different from Ruppeiner's in the volume factor as well as in the sign convention.

The thermodynamic Riemann curvature was first evaluated for several cases by Ruppeiner [2,3]. It is zero for monoatomic ideal classical gases, where there are no interparticle interactions. For many known models of interactions he noted the Gauss curvature $\xi_G=\frac{1}{2}R$ to be in excellent agreement with their correlation length. On the basis of such properties he suggested that the Riemann scalar curvature R is a measure of effective interactions (see Ruppeiner [4] for details), while Janyszek and Mrugala offered another interpretation [5]. They calculated the curvature for many known thermodynamical models [5–7], including the models worked out by Ruppeiner. For instance, for the 1D Ising mode [5] they reported that the R in the ferromagnetic case is larger than the R in the antiferromagnetic case. For ideal quantum gases [6], they showed that the R for ideal Fermi gases is always negative whereas for ideal Bose gases it is always positive and diverges as the temperature approaches zero. For a real gas [7], the R is positive and tends to infinity as the system approaches the critical point. Motivated by these properties, they suggested that the thermodynamic curvature is a measure of the stability. Namely, the smaller the R, the more stable the system.

C. Application to random or correlated-walk processes

We applied information geometry to nonequilibrium processes such as random or correlated walks. First we treated a RW model [8], in which a walker on a D-dimensional cubic lattice jumps from a site to one of the $2D$ nearest neighbors or stays at the same site with given jump probabilities. The probability arriving at a site on the lattice after N steps is characterized by the jump probabilities. We examined the curvature of the family of the arrival probabilities characterized by the jump parameters. Different from the thermodynamical cases, the statistical manifold develops with the step time N. We found an interesting result: the Riemann scalar curvature R approaches zero as the step time N increases. In the RW model, successive steps are not correlated with each other. Namely, the steps do not interact with each other. Thus this result corresponds to the same result as ideal classical gases. We noted also the decrease behavior of the R with the lapse of the step time. Regarding the RW process as a transition process from a localized unstable state to a stable equilibrium state, we suggested that the Riemann scalar curvature might be a measure of stability in nonequilibrium processes as well as in thermodynamic systems.

In successive papers [9,10], we applied the same technique to a CW model [13], in which a walker moves along a linear lattice of infinite extension right or left with given jump probabilities. The right and left steps are called steps of type 1 and 2, respectively. If the last step is of type j, the probabilities of stepping right or left are denoted by p_j and q_j with the normalization condition $p_j+q_j=1$. (Refer to Fig. 1, in which a more general model is traced.) The probability of arriving at a site on the linear lattice after N units of time is characterized by two independent jump probabilities, for instance, p_1 and q_2. We examined the curvature of the family of the arrival probabilities characterized by such two jump parameters, and found the fact that the 2D Riemann scalar curvature approaches -1 as the step time N increases. In the CW model, two successive steps are correlated with each other. Namely, the range of interactions between steps is of 1. Hence $|R|$ approaches the interaction length. We have already seen that the R of the RW model approaches 0. Those results suggest that Ruppeiner's interpretation of the Riemann scalar curvature as a measure of effective interactions may apply to the final states of stochastic processes such as random or correlated walks as well as thermodynamic systems.

Further we showed that the parameter space of the CW model evolves through some characteristic eras: it starts at a point, and changes to a line, and then to a homogeneous spherical surface of $R=\frac{1}{2}$. The homogeneous space immediately transforms to an inhomogeneous space. The inhomogeneity gradually grows: a region of the inhomogeneous space violently oscillates in time and another region expands fast. As a whole, the curvature of the space decreases and soon becomes negative. The oscillations have already started to fade away. The negative curvature goes on decreasing and finally the space converges to a homogeneous saddle surface of $R=-1$. Such a dynamical behavior of the curvature was shown to be well understood by the terms of stability and order parameter of stochastic processes.

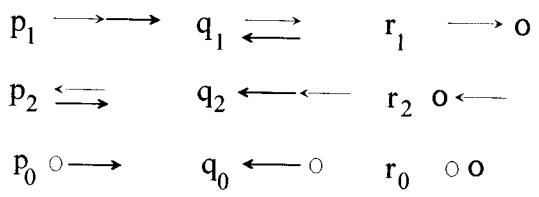

FIG. 1. Step probabilities with correlations. The thick arrows and circles correspond to the steps in question and the thin arrows and circles to the last steps. The direction of each arrow is the direction of jumping and each circle represents staying.

For instance, the asymptotic expression of R is as follows:

$$R=-1+h(p_1,q_2)/N \tag{17}$$

for large N. The inhomogeneity function $h(p_1,q_2)$ in the order N^{-1} is independent of the difference coordinate $\nu=(p_1-q_2)/2$, the asymmetry between rightward steps and leftward steps, and also the function monotonically decreases with respect to another coordinate $u=(p_1+q_2)/2$. Note that the u coordinate represents the orderliness of walks. In fact $u\to 1$ is equivalent to $p_2\to 0$ and $q_1\to 0$. Namely, the probabilities of stepping in a direction opposite to the previous step approach zero. So a walker of $u\sim 1$ tends to move almost without flip-flops. Namely, the walker moves smoothly and regularly. We may then regard the u coordinate as a regularity parameter or an order parameter. Hence the Riemann scalar curvature R is small for ordered states in the asymptotic time region. This consequence is consistent with the interpretation of Janyszek and Mrugala for the Riemann scalar curvature of thermodynamic systems.

III. STATISTICAL MANIFOLDS ASSOCIATED WITH A CORRELATED-WALK MODEL

Our interest is not in stochastic processes themselves but in statistical manifolds associated with them. We here take a known simple CW model used by Okamura *et al.* to discuss the atomic diffusion in metals with impurities [14,15]. In that model a walker correlatively moves or stays on a cubic lattice. The correlated walks on the 3D lattice are characterized by four independent transition probabilities of jump or stay. To reduce the number of independent transition probabilities, we think of the same walks on a linear lattice.

A. A model of walkers jumping or staying correlatively

Suppose that a walker moves along a linear lattice of infinite extension right or left with given jump probabilities or that the walker sometimes stays without jump. The right step, the left step, and the stay are called steps of type 1, 2, 0, respectively. If the last step is of type j, the probabilities of stepping right or left or staying are denoted by p_j, q_j, r_j with the normalization condition

$$p_j+q_j+r_j=1 \quad (j=1,2,0). \tag{18}$$

The definitions of the step probabilities are shown in Fig. 1, where the steps in question are indicated by thick arrows or circles, and the last steps by thin arrows or circles. Two

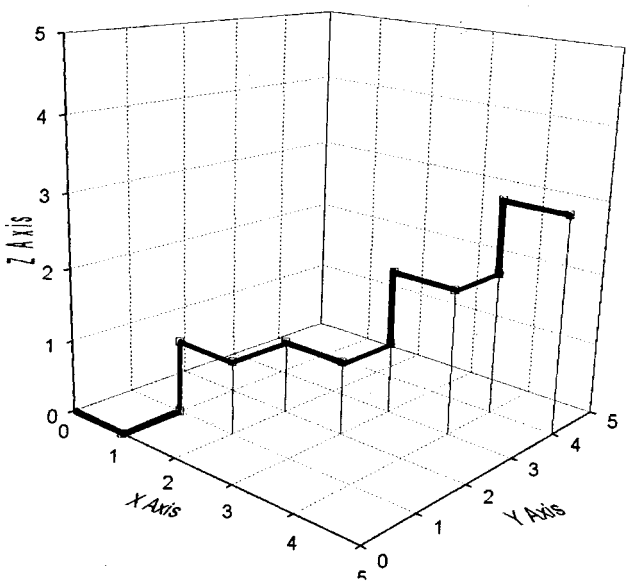

FIG. 2. Moves of a walker on a linear lattice can be represented by outward moves of an object on the first quadrant of the cubic lattice (X,Y,Z).

successive steps are correlative in the meaning that the step probabilities depend on the type j of the last steps.

The dynamics of the walker stepping correlatively on the linear lattice can also be represented in a cubic lattice. The walker's moves toward the right correspond to the X-ward moves of an object on the cubic lattice, the walker's moves toward the left to the Y-ward moves, and the walker's stay period to the Z-ward moves. (See Fig. 2.)

Let $P_j(X,Y,Z)$ be the probabilities of the object arriving at the site (X,Y,Z) with step type j after N units of time. The probability of the object arriving at (X,Y,Z) from any direction is

$$P(X,Y,Z)=P_1(X,Y,Z)+P_2(X,Y,Z)+P_0(X,Y,Z). \tag{19}$$

Because of $X+Y+Z=N$, we can regard P's as functions of X, Y, and N. The new functions are denoted by Q:

$$Q_j(X,Y,N)=P_j(X,Y,Z), \quad Q(X,Y,N)=P(X,Y,Z). \tag{20}$$

Consideration of two successive steps yields the following relations for P_j or Q_j:

$$\begin{aligned} Q_1(X,Y,N)&=p_1Q_1(X-1,Y,N-1)+p_2Q_2(X-1,Y,N-1)\\ &\quad +p_0Q_0(X-1,Y,N-1) \quad (X\geqslant 1,\ Y\geqslant 0,\ N\geqslant 1),\\ Q_2(X,Y,N)&=q_1Q_1(X,Y-1,N-1)+q_2Q_2(X,Y-1,N-1)\\ &\quad +q_0Q_0(X,Y-1,N-1) \quad (X\geqslant 0,\ Y\geqslant 1,\ N\geqslant 1),\\ Q_0(X,Y,N)&=r_1Q_1(X,Y,N-1)+r_2Q_2(X,Y,N-1)\\ &\quad +r_0Q_0(X,Y,N-1) \quad (X\geqslant 0,\ Y\geqslant 0,\ N\geqslant 1). \end{aligned} \tag{21}$$

These are the equations of motion for $Q_i(X,Y,N)$.

The probability function $Q(X,Y,N)$ produces the marginal distribution functions

$$Q(X,N)\equiv\sum_Y Q(X,Y,N), \quad Q(Y,N)\equiv\sum_X Q(X,Y,N). \tag{22}$$

The equations of motion for the marginal distribution functions can be easily obtained by summing the fundamental equations of motion about all values of X or Y.

Here we do not have any interest in solving these equations of motion exactly. Even though we have exact solutions, it is very difficult to calculate geometrical objects such as the metric tensor through formulas (1)–(13). Hence we will adopt a numerical method.

B. Statistical manifolds

Let S be a set of the probability functions $Q(X,Y,N)$ parametrized by the jump probabilities p_j,q_j,r_j:

$$S=\{Q(X,Y,N)\}. \tag{23}$$

Because of the normalization condition (18), each function $Q(X,Y,N)$ in S is specified by a 6D parameter $\theta=(\theta^1,\theta^2,\ldots,\theta^6)$ such as $(p_1,p_2,p_0,q_1,q_2,q_0)$. Since $Q(X,N)$ is sufficiently smooth in θ, the set S has the structure of a 6D manifold, where θ plays the role of a coordinate system.

In the same way, we write $S^{(m)}$ for a 6D space of the marginal probability functions parametrized by the jump probabilities p_j,q_j,r_j:

$$S^{(m)}=\{Q(X,N)\} \text{ or } \{Q(Y,N)\}. \tag{24}$$

Numerical calculation of the curvature tensor of 6D spaces requires a lot of computer resources. Hence let us restrict our consideration to 3D subspaces induced by symmetric walk:

$$p_1=q_2, \quad p_2=q_1, \quad p_0=q_0. \tag{25}$$

These conditions and the normalization condition produce another symmetric relation;

$$r_1=r_2. \tag{26}$$

A function in the subspaces

$$S_{\mathrm{SW}}=\{Q(X,Y,N)|p_1=q_2,\ p_2=q_1,\ p_0=q_0\}, \tag{27}$$

$$S^{(m)}_{\mathrm{SW}}=\{Q(X,N)|p_1=q_2,\ p_2=q_1,\ p_0=q_0\}, \tag{28a}$$

or

$$S^{(m)}_{\mathrm{SW}}=\{Q(Y,N)|p_1=q_2,\ p_2=q_1,\ p_0=q_0\} \tag{28b}$$

is specified by a 3D parameter such as (p_1,p_2,p_0), that is, the function is characterized by two jump parameters and a stay parameter.

Let us now foliate the 3D space S_{SW} by the stay parameter r_0. The foliation

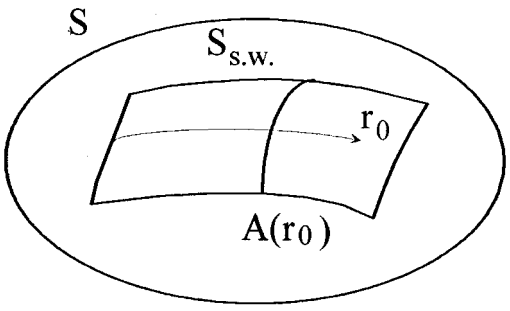

FIG. 3. Sketch of the relation among the three spaces S, S_{SW}, and $A(r_0)$, whose elements are the probability distribution functions $Q(X,Y,N)$. The relation of the spaces $S^{(m)}$, $S_{\mathrm{SW}}^{(m)}$, and $A^{(m)}(r_0)$ also are all the same except that their elements are the marginal probability distribution functions $Q(X,N)$ [or $Q(Y,N)$].

$$S_{\mathrm{SW}}=\bigcup_{0\leqslant r_0\leqslant 1} A(r_0) \tag{29}$$

is a partitioning of S_{SW} into 2D spaces $A(r_0)$. In the same way the 3D space $S_{\mathrm{SW}}^{(m)}$ is foliated:

$$S_{\mathrm{SW}}^{(m)}=\bigcup_{0\leqslant r_0\leqslant 1} A^{(m)}(r_0). \tag{30}$$

See Fig. 3.

In the present paper we treat entirely the most simple case, that is, the 2D subspace $A^{(m)}(r_0)$ of marginal probability distribution functions. Details including other cases will be reported elsewhere.

C. A method of numerical analysis

The equations determining the marginal distribution function $Q(X,N)$ in $A^{(m)}(r_0)$ are easily obtained by summing the fundamental equations of motion about all values of Y and applying the symmetry condition,

$$\begin{aligned}
Q_1(X,N)&=aQ_1(X-1,N-1)+\beta Q_2(X-1,N-1)\\
&\quad+p_0Q_0(X-1,N-1)\quad (X\geqslant 1,\ N\geqslant 1),\\
Q_2(X,N)&=\beta Q_1(X,N-1)+aQ_2(X,N-1)\\
&\quad+p_0Q_0(X,N-1)\quad (X\geqslant 0,\ N\geqslant 1),\\
Q_0(X,N)&=\gamma Q_1(X,N-1)+\gamma Q_2(X,N-1)\\
&\quad+r_0Q_0(X,N-1)\quad (X\geqslant 0,\ N\geqslant 1),
\end{aligned} \tag{31}$$

with $a\equiv p_1=q_2$, $\beta\equiv p_2=q_1$, $\gamma\equiv 1-a-\beta$, and $2p_0=1-r_0$. The equations of motion for $Q(Y,N)$ are given by replacing X by Y and changing a and β. Therefore the space of $Q(X,N)$ is equivalent to the space of $Q(Y,N)$. The coordinates a and β only interchange in both spaces. In the following, $A^{(m)}(r_0)$ stands for the space of $Q(X,N)$.

Let us calculate the Riemann scalar curvature R on $A^{(m)}(r_0)$ by the numerical method proposed in [9]. The new method treats the basic recursive relations and their parameter derivatives together. In the usual method using only the basic equations of motion, it is necessary to evaluate the recursive equation at three neighboring points at least, because R contains probability functions and their parameter derivatives up to the second derivative.

We successively solve these recursive relations and their parameter derivatives together. We use the coordinate system $(a,\beta)\equiv(p_1,p_2)$ for a while. Iterative calculation of the basic recursive relations and their derivatives gives the Riemann scalar curvature R at each step through Eqs. (1)–(9). Of course, any other coordinate system should produce the same value of the scalar R.

D. Numerical solutions

We have numerically evaluated the Riemann scalar curvature R on the leaves $A_{\mathrm{SW}}^{(m)}(r_0)$, $0\leqslant r_0\leqslant 1$. These 2D spaces nucleate at $N=2$, as will be explained below.

Suppose that a walker starts from a state localized upon a point at $N=0$. Whatever initial values are assigned to $Q_1(0,0)$, $Q_2(0,0)$, and $Q_0(0,0)$, we have then $Q(0,0)=1$. This expression leads to $g_{11}=g_{22}=g_{12}=0$. Hence the $N=0$ space does not extend to any direction or it degenerates to a point.

At $N=1$, as far as a walker starts from a state localized upon a point at $N=0$, we have

$$\begin{aligned}
&Q(0,1)+Q(1,1)=1,\\
&Q(X,1)=0,\quad X\geqslant 2.
\end{aligned} \tag{32}$$

Both $Q(0,1)$ and $Q(1,1)$ are functions of coordinates p_1 and p_2. It is possible to take one of the two functions as a coordinate transformation, for instance, $\theta^1=Q(0,1)$. We then adopt a function independent of $Q(0,1)$ as another coordinate θ^2. The new coordinate system results in $g_{11}=1/[\theta^1(1-\theta^1)]$, $g_{22}=g_{12}=0$. Thus the $N=1$ space also has no extension to the θ^2 direction or it degenerates to a line.

At the first nondegenerate time $N=2$, the space has the constant positive Riemann scalar curvature $R=\frac{1}{2}$. This can be proved as follows:

$$\begin{aligned}
&Q(0,2)+Q(1,2)+Q(2,2)=1,\\
&Q(X,2)=0,\ X\geqslant 3.
\end{aligned} \tag{33}$$

Any of $Q(0,2)$, $Q(1,2)$, and $Q(2,2)$ is a function of p_1 and p_2. It is convenient to take two functions of them, for instance, $\theta^1=Q(1,2)$ and $\theta^2=Q(2,2)$ as new coordinates. The metric tensors in the new coordinate system are as follows:

$$\begin{aligned}
g_{11}&=\frac{1}{1-\theta^1-\theta^2}+\frac{1}{\theta^1},\quad g_{22}=\frac{1}{1-\theta^1-\theta^2}+\frac{1}{\theta^2},\\
g_{12}&=\frac{1}{1-\theta^1-\theta^2}.
\end{aligned} \tag{34}$$

It is a simple exercise to ascertain that the metric yields $R=\frac{1}{2}$. This curvature is displayed in Fig. 4. Here we should note the restriction

$$p_1+p_2\leqslant 1\quad \text{or}\quad a+\beta\leqslant 1, \tag{35}$$

because $0\leqslant\gamma=1-a-\beta\leqslant 1$.

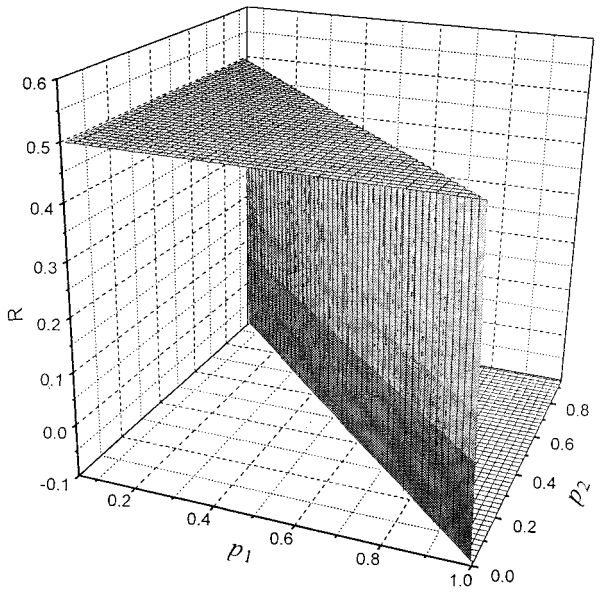

FIG. 4. Riemann scalar curvature R at $N=2$.

At $N>2$, we have investigated the time development of R at a typical point under a typical initial condition about many leaves. Figures 5(a) and 5(b) show $R\rightarrow -1$ $(0\leqslant r_0<1)$ and $R\rightarrow \frac{1}{2}$ $(r_0=1)$ at the point under the initial condition. These limit values are easily imagined to be independent of the initial value, because the distribution function $Q(X,N)$ loses the initial characteristics as the step time N goes by [16]. However, we do not know whether the limit values of R depend on the coordinate value. So we investigated the time development of several leaves. The time development of two typical leaves $r_0=0$ and 1 is displayed in Figs. 6 and 7. These figures show that the homogeneous space at $N=2$ immediately deforms but again approaches the homogeneous space $R=-1$ for $r_0=0$ or $\frac{1}{2}$ for $r_0=1$. We have ascertained that all leaves except $r_0=1$ converge to the same homogeneous space of $R=-1$. Namely, we conclude

$$R\rightarrow -1 \quad (0\leqslant r_0<1), \qquad R\rightarrow \tfrac{1}{2} \quad (r_0=1). \tag{36}$$

The first equation suggests the final distribution functions to be normal distribution functions, because the family of 1D normal distribution functions with two parameters such as mean and variance is known to constitute a saddle surface of $R=-1$ [11]. To prove whether this inference is right, we have numerically calculated the distribution functions at many points of many leaves, and we have ascertained

$$Q(X,N)\rightarrow (2\pi\sigma^2)^{1/2}\exp\left(-\frac{(X-m)^2}{2\sigma^2}\right) \quad (0\leqslant r_0<1) \tag{37}$$

for large N. Figure 8 is an example, which shows that the $Q(X,N)$ at $N=1000$ is in excellent agreement with the normal distribution function (37).

We have calculated the distribution functions at many points of the leaf $r_0=1$ as well, and found these distribution functions are represented by

$$Q(X,N)\rightarrow \eta\delta(X)+\xi e^{-\lambda X} \tag{38}$$

for large N. The normalization condition of probability leads to

$$\eta+\frac{\xi}{e^{-\lambda}-1}=1. \tag{39}$$

Figure 9 is an example, which shows that the $Q(X,N)$ at $N=1000$ is in excellent agreement with the probability distribution function (38).

We now have the analytical expressions (37) and (38) for the probability distribution functions. Then we can analytically calculate the a curvature. Since the family of normal distribution functions belongs to the exponential family (10), we have immediately

$$R^{(1)}_{ijkl}\rightarrow 0 \quad (0\leqslant r_0<1). \tag{40}$$

The calculation of the a curvature of the leaf $r_0=1$ is somewhat troublesome. We have taken advantage of a symbolic formula manipulation program [17]. The details of calculation are given in the Appendix. The a-curvature tensor is

$$R^{(a)}_{ijkl}\rightarrow (1-a^2)\,\frac{e^{\lambda}}{4(1-e^{\lambda}+\xi)(1-e^{\lambda})^3}\,(\delta_{ik}\delta_{jl}-\delta_{il}\delta_{jk}) \tag{41}$$

in the (ξ,λ) coordinate system. Therefore the leaf of $r_0=1$ as well as the leaves of $0\leqslant r_0<1$ are flat at $a=1$.

IV. DISCUSSION

We discuss the asymptotic properties of the Riemann scalar curvature (36) from three different points of view and the dynamic behavior of that.

Let us first discuss the asymptotic property of the Riemann scalar curvature from the viewpoint of walk trajectories. The walker of $r_0\neq 1$ may stop temporarily but jumps right or left again. So the path extends infinitely. On the other hand, once the walker of $r_0=1$ stops at a site, the walker is trapped there forever, and the path extends finitely. In other words, the paths of $r_0\neq 1$ are continuous, while the paths of $r_0=1$ are discontinuous or terminated. Thus we can say that the Riemann scalar curvature R associated with continuous paths is smaller than the R associated with discontinuous paths. Generally speaking, the more regular a path, the smaller the R. This statement is consistent with our conclusion in a previous paper [9], which is briefly summarized in Sec. II C.

Secondly we show that the Riemann scalar curvature R's for the $r_0=1$ statistics and the $r_0=0$ statistics are very similar to the R's for Bose-Einstein statistics (BE) and Fermi-Dirac statistics (FD), respectively. The walker of $r_0=1$ stays at a site for infinite time, while the walker of $r_0=0$ stays at most for one step time. If it is allowed to make the stay time correspond to the occupation number in quantum statistics, the $r_0=1$ statistics then corresponds to BE in which the number of particles occupying a state is unlimited, and the $r_0=0$ statistics corresponds to FD in which the occupation number is at most one. Janyszek and Mrugala [6] showed that the thermodynamic Riemann scalar curvature

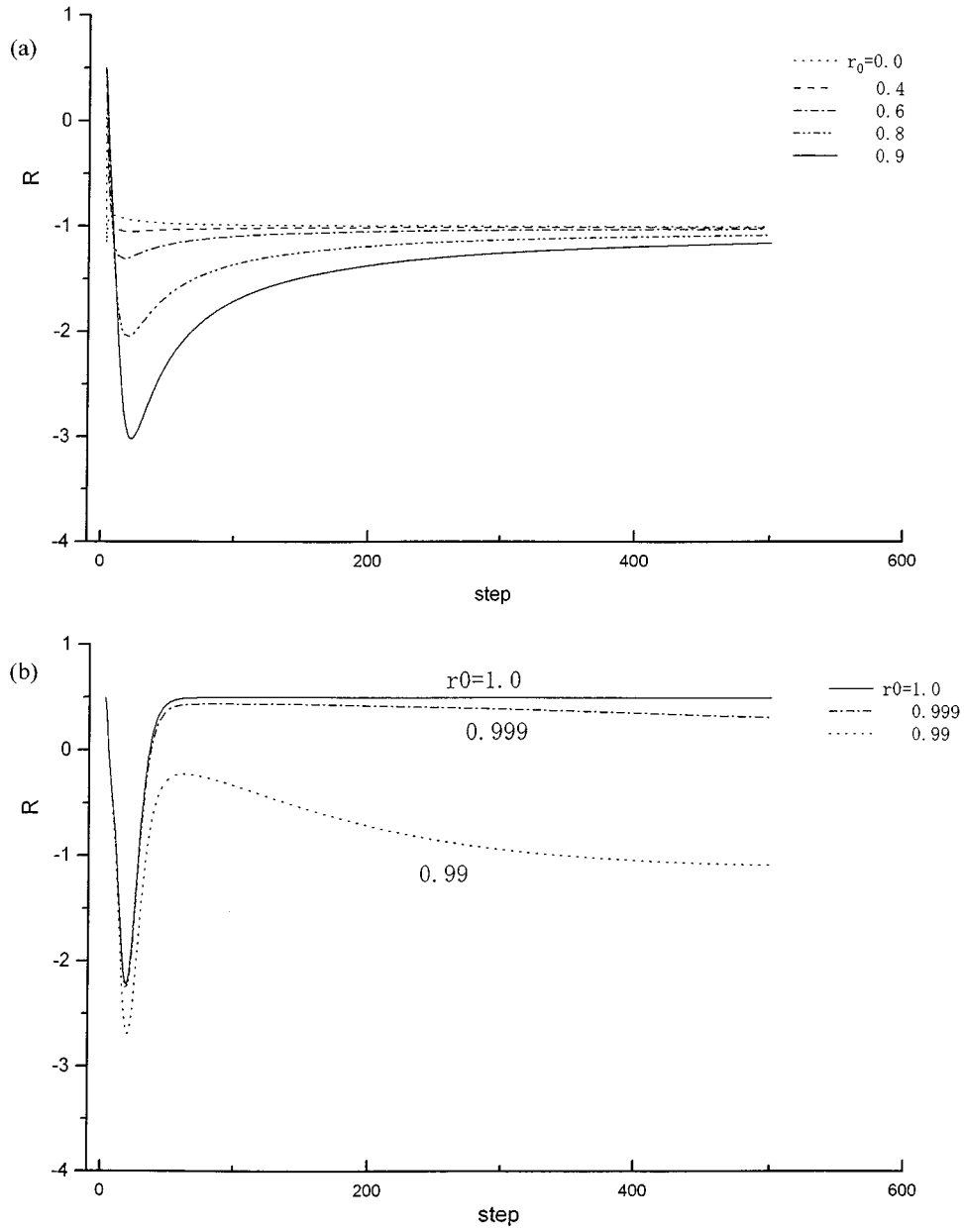

FIG. 5. Time development of the Riemann scalar curvature R at the coordinate $(p_1,p_2)=(0.4,0.4)$ under the initial condition $Q_1(0,0)=Q_2(0,0)=0.5$: (a) $r_0=0.0,04,0.6,0.8,0.9$; (b) $r_0=0.99,0.999,1.0$.

R is positive for BE and negative for FD. Namely, R for BE is larger than R for FD. According to such results, they proposed to understand the R as a measure of stability, because a Fermi gas, with the effectively repulsive interactions, is more stable than any Bose gas, with the effectively attractive interactions. If we accept their interpretation, we can say, from the correspondence, that the $r_0=0$ system ($R=-1$) is more stable than the $r_0=1$ system ($R=\frac{1}{2}$). The statement seems to be reasonable, because the distribution functions (38) at $r_0=1$ are different in kind from those in the range $0\leqslant r_0<1$, which are normal distribution functions. Hence, under a small change of r_0, the distribution functions around $r_0=1$ largely change, but the distribution functions around $r_0=0$ remain in the same family.

We want to note that the CW models of $r_0=1$ and 0 are similar to BE and FD in the values of R as well as in the sign of R. Janyszek and Mrugala gave a table of the R for chosen values of the fugacity η for bosons and fermions (see Table 1 in Ref. [6]). The table shows that the R for fermions largely changes in the range of $0.100<\eta<0.990$. For instance, the R at $\eta=0.9$ becomes five orders in magnitude larger than the R at $\eta=0.1$. To check the large changes, we recalculated the R using formulas (4.17) and (4.21) of Ref. [6]. The calculation reproduced the same result for bosons but a quite different result for fermions. Our numerical result is given in Table I. It should be noted that Janyszek and Mrugala tabulated the R in units of $20\lambda^3V^{-1}$ for bosons and in units of $20\lambda^3V^{-1}(2s+1)^{-1}$ for fermions. The λ is the thermal wavelength and s is the spin. We used units without the numerical factor 20 for the convenience of comparing the quantum gas systems. The table shows that the R for fermions is about -0.2, while the R for bosons slowly increases from about 0.2 (at $\eta=0.1$) to 1.2 (at $\eta=0.99$). The mean value is about 0.5. Hence the CW models of $r_0=1$ and 0 are similar to BE and FD in the values of R as well in the sign. However, there is a decisive difference; the R for bosons becomes infinite for $\eta\rightarrow 1$, while the R of the $r_0=1$ statistics is the constant of $\frac{1}{2}$.

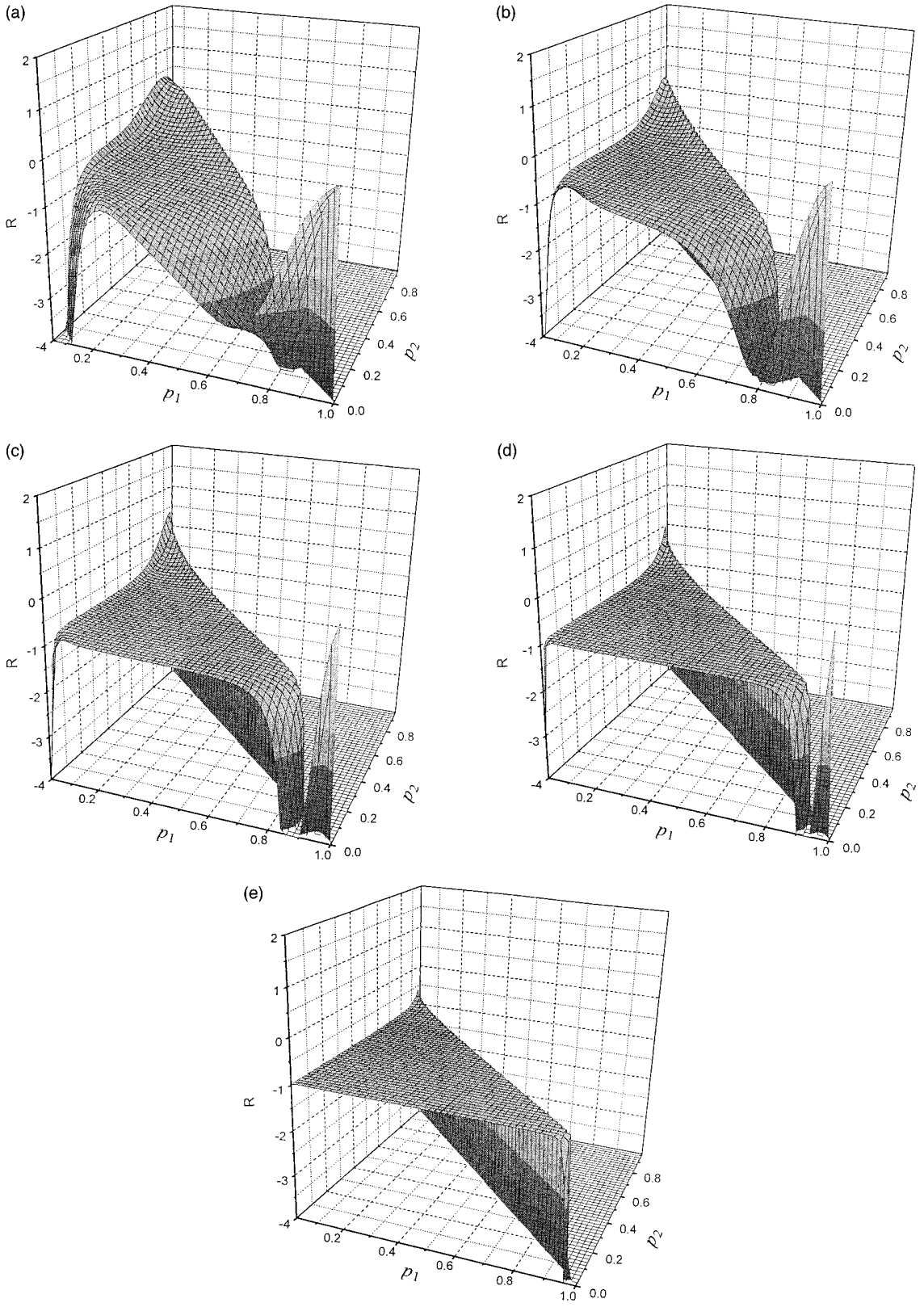

FIG. 6. Time development of the Riemann scalar curvature R of the leaf $r_0=0$: (a) $N=10$, (b) $N=20$, (c) $N=50$, (d) $N=100$, and (e) $N=300$.

As the third asymptotic property of the R we note the fact that the CW models investigated here and in a previous paper have a property common to thermodynamic systems. We have seen that the $a=1$ curvature of the CW models is zero for $N\rightarrow\infty$ or approaching equilibrium states. In particular, the equilibrium distribution function (38) for the $r_0=1$ model should be noted not to be a member of the exponential family (10). As has been noted in Sec. II, any thermody-

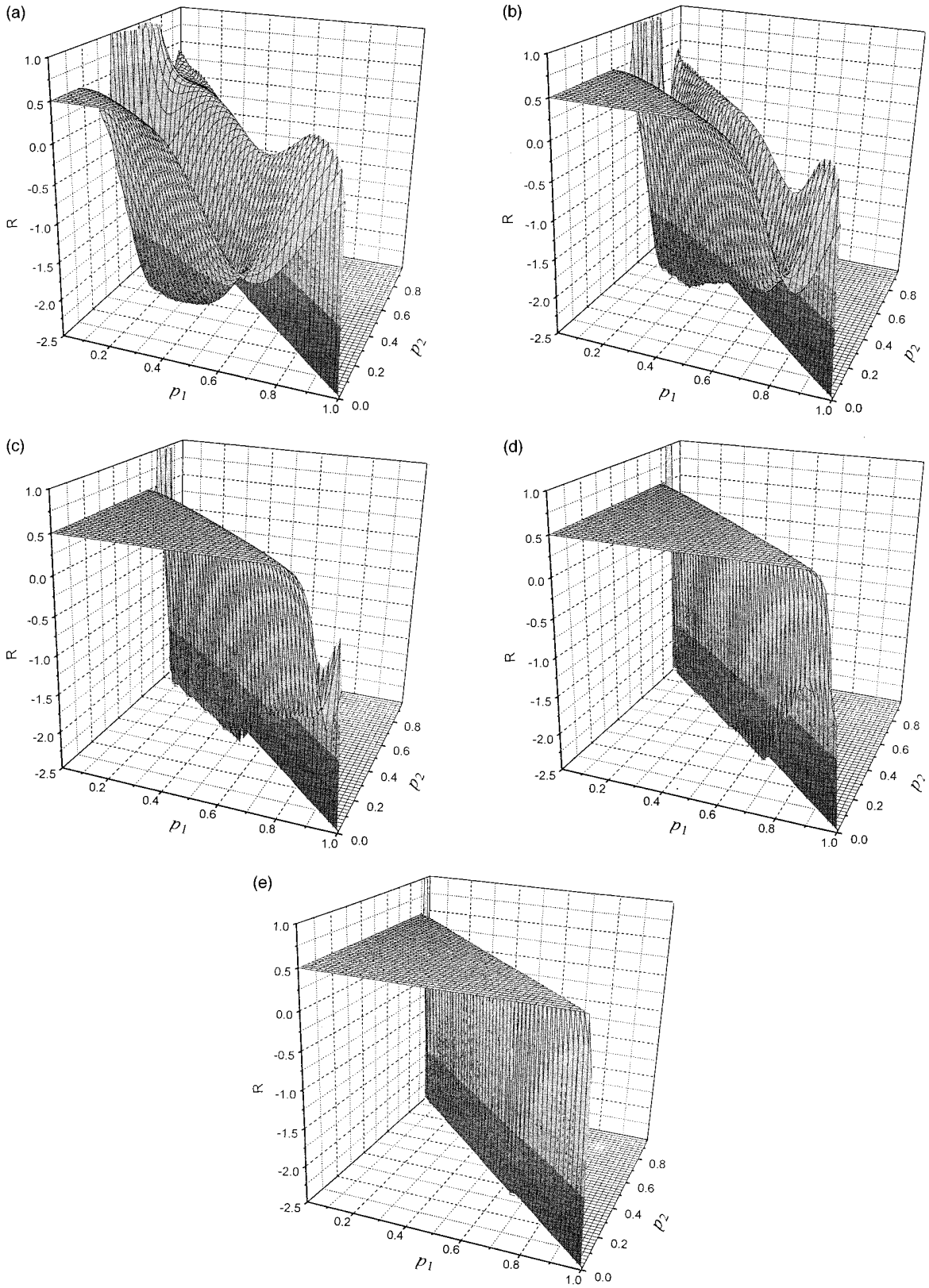

FIG. 7. Time development of the Riemann scalar curvature R of the leaf $r_0=1$: (a) $N=10$, (b) $N=20$, (c) $N=50$, (d) $N=100$, and (e) $N=300$.

namic system has zero $a=1$ curvature as an inevitable consequence of the fact that the distribution function is a member of an exponential family. This fact seems to suggest that the zero $a=1$ curvature might be a universal property in a broader class of equilibrium systems including thermodynamic systems.

Next we proceed to discuss the dynamic behavior of the Riemann scalar curvature R. Figures 5(a) and 5(b) show that

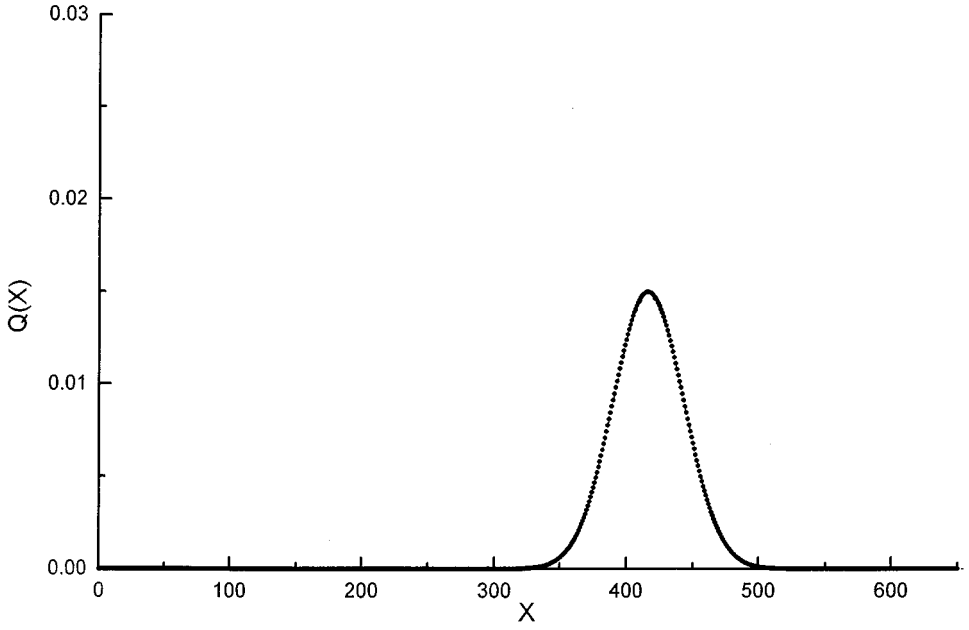

FIG. 8. Marginal probability distribution function $Q(X) \equiv Q(X,N)$ at $N=1000$, $(p_1,p_2) = (0.7,0.2)$, $r_0=0.5$ under the initial condition $Q_1(0,0)=Q_2(0,0) = 0.5$. The dotted line stands for $Q(X)$ and the dashed line for the normal distribution function $N(m,\sigma)$ of mean $m=416.15$ and variance $\sigma=53.16$.

the R starts at $\frac{1}{2}$ and rapidly decreases for a short time. After that, R turns to increasing and finally approaches the equilibrium value $\frac{1}{2}$ or -1. It is possible to understand the early behavior by the interpretation of the R as a measure of stability. We suppose that any walker starts from a state localized upon a point. Such a localized distribution function rapidly spreads for a while, in general. Namely, the initial state is unstable. However, we could not find a satisfactory explanation of the increase behavior of the R.

Figures 6 and 7 display other remarkable features in the dynamic process of the Riemann scalar curvature. Figure 6 shows that there is a valley in the leaf $r_0=0$. In the other side of the valley, the R is almost homogeneous. In this side there appears a sharp-pointed mountain. As the step time N goes by, the almost homogeneous region gradually extends, and becomes more and more homogeneous. The mountain becomes increasingly sharp and thin. Finally the peak fades away. Figure 7 also shows that there is a valley in leaf $r_0 = 1$, which is parallel to the diagonal boundary line $p_1+p_2 = 1$ connecting the near corner and the far corner of the p_1-p_2 plane. The flat plane on the left side of the valley is a homogeneous region of $R=\frac{1}{2}$. As the step time N goes by, the homogeneous region extends and gradually suppresses the valley. Finally the homogeneous region swallows the valley, that is, the valley vanishes.

Now we show that the dynamic characteristic of the Riemann scalar curvature of $r_0=0$ is related to the existence of a runaway component that is a sharp peak at the edge of the skirts of a diffusive maximum in probability distribution functions. The existence of such a runaway component was found in a model equivalent to the special case $\gamma=r_0=0$ of Eq. (31) by Okamura *et al.* [18,19]. They gave the exact solutions with a specific initial condition, and showed that the solutions have a runaway component that is associated

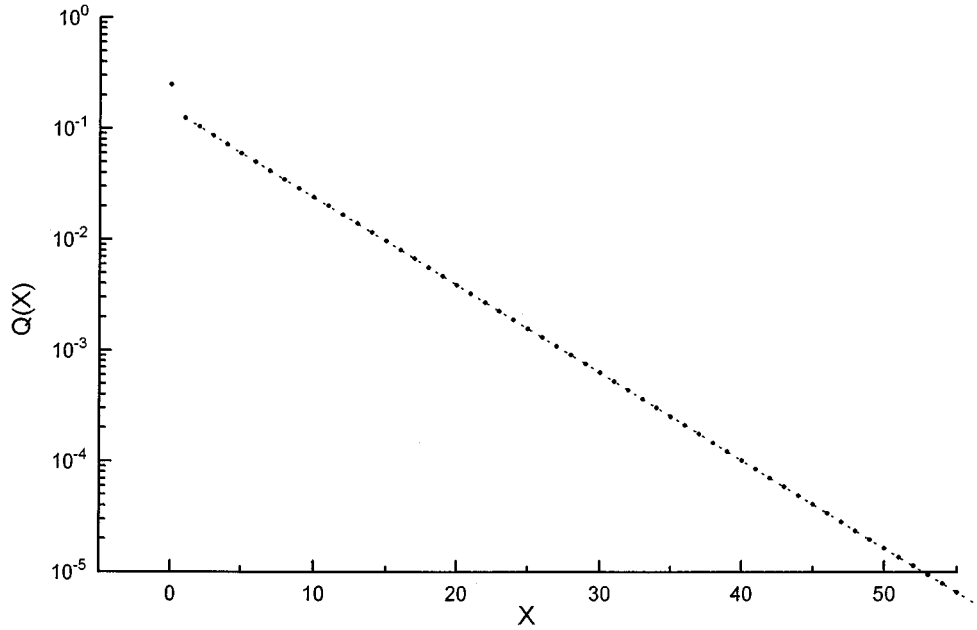

FIG. 9. Marginal probability distribution function $Q(X) \equiv Q(X,N)$ at $N=1000$, $(p_1,p_2) = (0.7,0.2)$, $r_0=1$ under the initial condition $Q_1(0,0)=Q_2(0,0) = 0.5$. The dotted line stands for $Q(X)$ and the dashed line for the probability distribution function (38) of $\eta=0.25$, $\xi=0.15$, and $\lambda=5.484\,81$.

TABLE I. Riemann scalar curvature R for chosen values of the fugacity η for bosons (in units of $\lambda^3 V^{-1}$ and fermions [in units of $\lambda^3 V^{-1}(2s+1)^{-1}$].

	Riemann scalar curvature R	
η	Bosons	Fermions
0.100	0.2270	−0.2158
0.300	0.2426	−0.2073
0.500	0.2669	−0.2005
0.700	0.3122	−0.1950
0.900	0.4594	−0.1903
0.910	0.4782	−0.1901
0.920	0.5025	−0.1899
0.930	0.5270	−0.1897
0.940	0.5605	−0.1895
0.950	0.6035	−0.1893
0.960	0.6615	−0.1891
0.970	0.7465	−0.1889
0.980	0.8890	−0.1887
0.990	1.2115	−0.1885

with free passage. Recently Okamura and Miyamoto [20] pointed out the fact that the existence of the runaway component does not come from the specific initial condition but from the correlation between steps itself. They then showed that the time when the runaway component is swallowed by the diffusive maximum is given by

$$N=\frac{1-2\delta+5\delta^2}{(1-\delta)^2} \tag{42}$$

in the case of $\gamma=r_0=0$, that is, $p_1+p_2=1$ and $r_0=0$. The δ expresses the degree of correlation, defined by

$$\delta=p_1-p_2. \tag{43}$$

For instance, $N=10$ for $(p_1,p_2)=(0.8,0.2)$, $N=65$ for (0.9,0.1), and $N=325$ for (0.95,0.05). Figures 6(a), 6(c), and 6(e) show that these positions are around the valley. Hence the valley is expected to be a transition region separating a purely diffusive region and a runaway region. To ascertain the expectation, we draw a contour-line map of the R at $N=50$ and a typical distribution function in each region. The white region in Fig. 10 corresponds to the valley in Fig. 6. On the left side of the white region where δ is small, the distribution function is a normal distribution. On the right side, the distribution function has a runaway component. In the white region separating the two regions, the distribution function does not have a flat skirts at the foot of the diffusive maximum. As time goes by, the white region is absorbed by the right side corner. Hence we can say that soon after the runaway component is swallowed by the diffusive maximum, the Riemann scalar curvature becomes a homogeneous value $R=-1$.

In the case of $r_0=1$, the dynamic characteristic of the Riemann scalar curvature is related to the existence of a diffusive maximum. To see it, we draw a contour-line map of

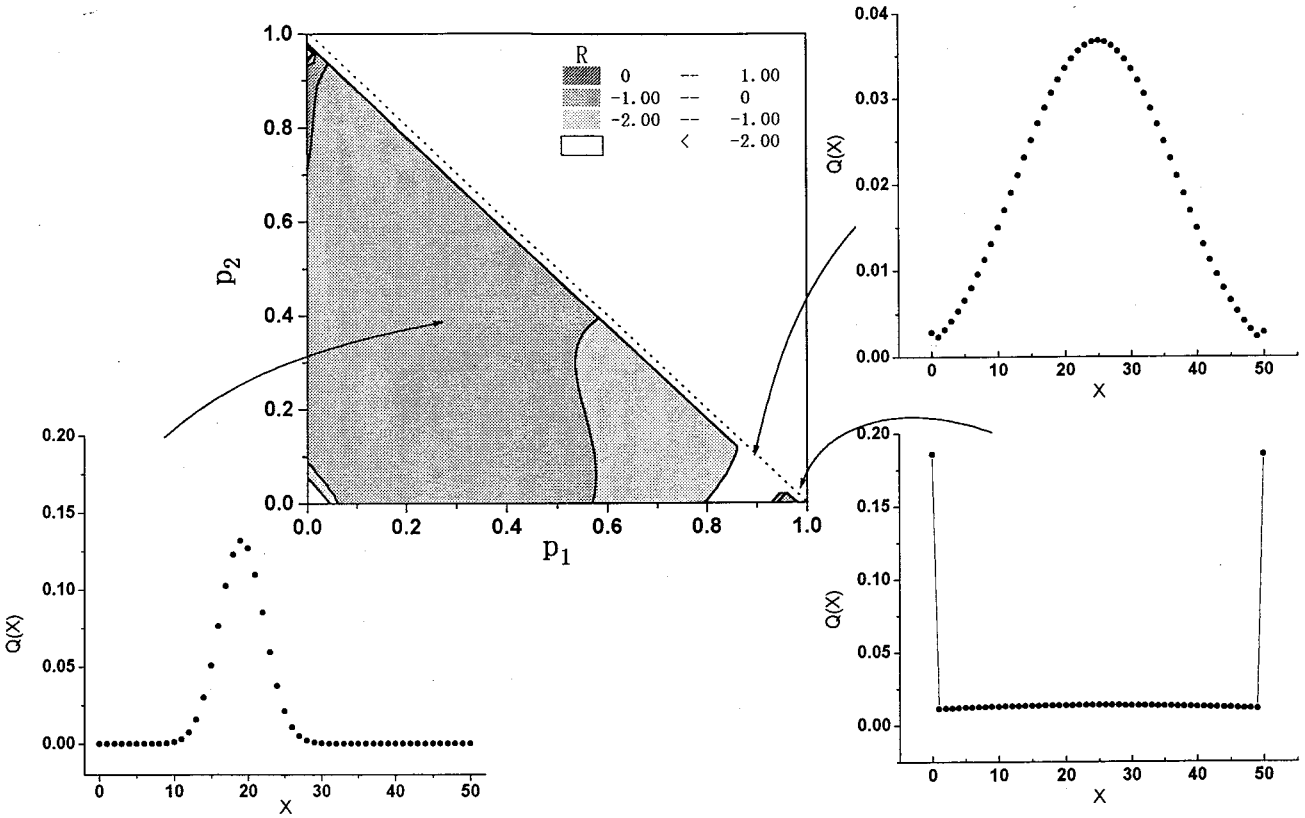

FIG. 10. Contour map of the Riemann scalar curvature R of the leaf $r_0=0$ at $N=50$, and the probability distribution functions $Q(X)$ at some points $(p_1,p_2)=(0.3,0.4),(0.9,0.1),(0.98,0.02)$.

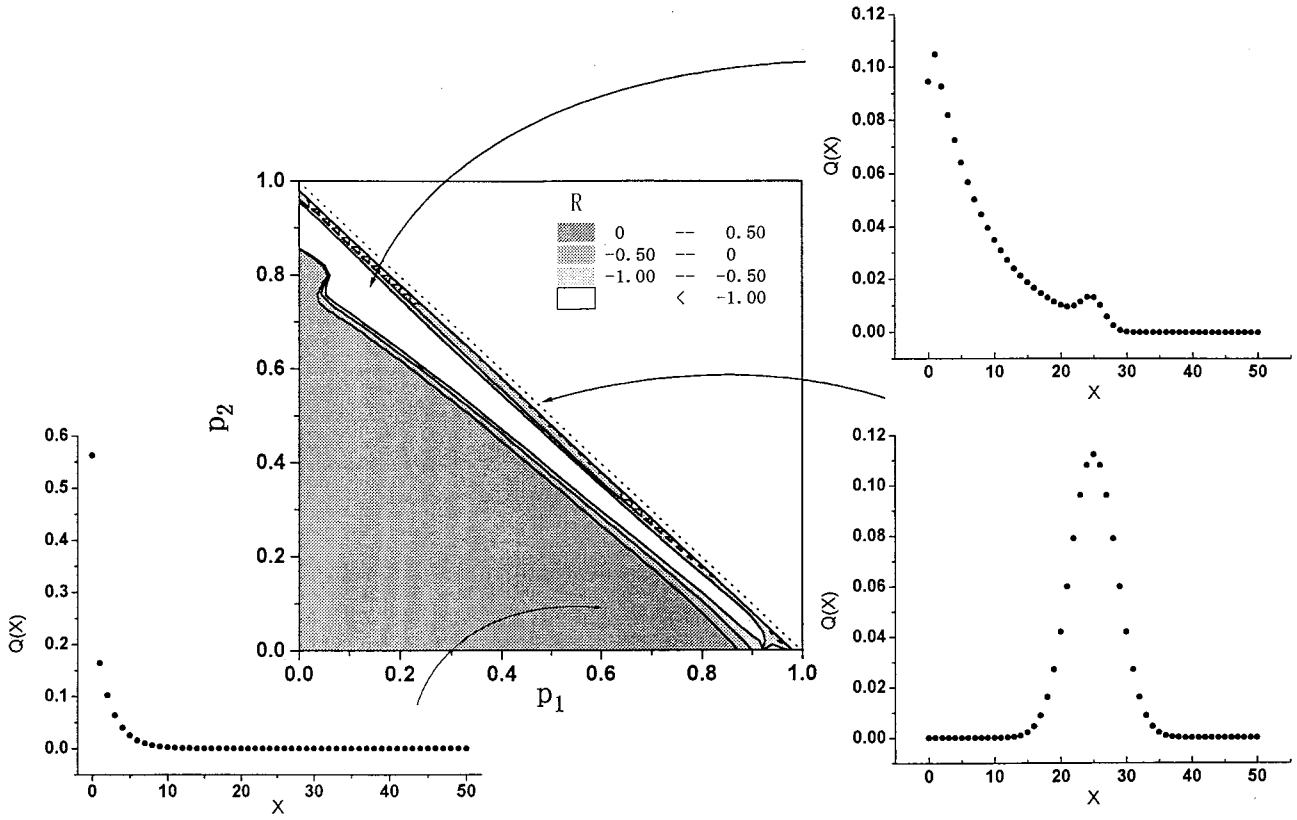

FIG. 11. Contour map of the Riemann scalar curvature R of the leaf $r_0=1$ at $N=50$, and the probability distribution functions $Q(X)$ at some points $(p_1,p_2)=(0.6,0.1),(0.18,0.76),(0.5,0.5)$.

the R at $N=50$ and a typical distribution function in each region. (See Fig. 11.) On the left side of the valley, the distribution function has a peak at $X=0$ and exponentially decays, which is described by Eq. (38). On the right side of the valley, the function is a normal distribution. In the bottom of the valley we see a mixture of an exponential function and a normal distribution function, and the peak at $X=0$ vanishes. The difference of the distribution functions in the three regions can be explained by the stepping activity $1-r_1=p_1+p_2$. Around the origin $(p_1,p_2)=(0,0)$, the activity is small, so such a walker is immediately trapped. In other words, the distribution function concentrates around $X=0$. Near the border the stepping activity is about 1, so such walkers might diffuse to far sites. Hence the distribution function is expected to be a normal distribution. In the white region separating the two regions, the walker has the step activity of some extent. Then the walker might diffuse up to some distance but the walker be trapped before long. Hence the distribution function is expected to have a diffusive maximum on the way of exponential decaying. In other words, it is a mixture of a exponential-decaying function and a diffusive maximum. As time goes by, the white region is absorbed by the diagonal border. Hence we can say that soon after the diffusive maximum is trapped, the Riemann scalar curvature becomes a homogeneous value $R=\frac{1}{2}$.

Finally we mention an interesting statistics which connects $r_0=0$ and 1 statistics, that is, an interpolative statistics. In the CW model, the $r_0=0$ statistics and the $r_0=1$ statistics are already connected by the continuous parameter $0\leqslant r_0\leqslant 1$. We have already shown that the R in the intermediate range is independent of r_0, and that the R takes the same value as the R of the $r_0=0$. The correspondence between the CW model and quantum statistics suggests examining the R for interpolative statistics relating FD and BE. We plan to report on this problem elsewhere in the near future.

ACKNOWLEDGMENTS

We would like to thank Dr. Y. Okamura for valuable comments and discussions. This work is supported in part by the Grant-in-Aid for Scientific Research from the Ministry of Education, Science, Sports and Culture (Grant No. 07680320).

APPENDIX: g_{ij}, g^{ij}, T_{ijk}, R_{ijkl} ASSOCIATED WITH THE PROBABILITY DISTRIBUTION FUNCTION (38)

In the coordinate system (ξ,λ),

$$g_{11}=\frac{1}{\xi(e^{\lambda}-1-\xi)},$$

$$g_{12}=\frac{-e^{\lambda}}{(e^{\lambda}-1)(e^{\lambda}-1-\xi)},$$

$$g_{22}=\frac{\xi e^{\lambda}(e^{2\lambda}-1-\xi)}{(e^{\lambda}-1)^3(e^{\lambda}-1-\xi)},$$

$$g^{11}=\xi\left[\frac{2f-1}{(f-1)^2}-\xi\right],$$

$$g^{12}=\frac{1}{(f-1)^2},$$

$$g^{22}=\frac{1}{\xi f(f-1)^2},$$

$$T_{111}=\frac{1}{(\eta+\xi)^2}(1-f)^3+\frac{1}{\xi^2}(f-1),$$

$$T_{112}=\frac{1}{(\eta+\xi)^2}\xi f(f-1)^3-\frac{1}{\xi}f(f-1),$$

$$T_{122}=\frac{1}{(\eta+\xi)^2}\xi^2 f^2(f-1)^3+f(f-1)(2f-1),$$

$$T_{222}=\frac{1}{(\eta+\xi)^2}\xi^3 f^3(f-1)^3-\xi f(f-1)(6f^2-6f+1),$$

$$R^{(0)}_{1212}=\frac{1}{4}\frac{e^\lambda}{(1-e^\lambda)^3(1-e^\lambda+\xi)},$$

$$\frac{1}{4}g^{mn}(T_{m11}T_{n22}-T_{m12}T_{n12})=-R^{(0)}_{1212},$$

$$\frac{-1}{2}(\nabla^{(0)}_k T_{ijl}-\nabla^{(0)}_l T_{ijk})=0,$$

$$R^{(a)}_{ijkl}=\frac{1-a^2}{4}\frac{e^\lambda}{(1-e^\lambda)^3(1-e^\lambda+\xi)}(\delta_{ik}\delta_{jl}-\delta_{il}\delta_{jk}).$$

[1] R. S. Ingarden, Y. Sato, K. Sugawa, and M. Kawaguchi, Tensor, N. S. **33**, 347 (1979).
[2] G. Ruppeiner, Phys. Rev. A **20**, 1608 (1979).
[3] G. Ruppeiner, Phys. Rev. A **24**, 488 (1981).
[4] G. Ruppeiner, Rev. Mod. Phys. **67**, 605 (1995).
[5] H. Janyszek and R. Mrugala, Phys. Rev. A **39**, 6515 (1989).
[6] H. Janyszek and R. Mrugala, J. Phys. A **23**, 467 (1990).
[7] H. Janyszek, J. Phys. A **23**, 477 (1990).
[8] T. Obata, H. Hara, and K. Endo, Phys. Rev. A **45**, 6997 (1992).
[9] T. Obata, H. Hara, and K. Endo, J. Phys. A **27**, 5715 (1994).
[10] T. Obata and H. Hara, InterDisciplinary Inf. Sci. **2**, 111 (1996).
[11] S. Amari, in *Differential-Geometrical Methods in Statistics*, edited by D. Brillinger, S. Fienberg, J. Gani, J. Hartigan, and K. Krickeberg, Lecture Notes in Statistics Vol. 28 (Springer, New York, 1985).
[12] C. W. Misner, K. S. Thorne, and J. A. Wheeler, *Gravitation* (Freeman, San Francisco, 1973).
[13] S. Fujita, *Statistical and Thermal Physics I. Probabilities and Statistics, Thermodynamics and Classical Statistical Mechanics* (Krieger, Malabar, FL, 1986), Chap. 2.
[14] S. Fujita, *Statistical and Thermal Physics II. Quantum Statistical Mechanics and Simple Applications* (Krieger, Malabar, FL, 1986), Chap. 13.
[15] Y. Okamura, E. Blaisten-Barojas, S. Fujita, and S. V. Godoy, Phys. Rev. B **22**, 1638 (1980).
[16] Y. Okamura (private communication).
[17] MATHEMATICA for MS Windows, Version 2.2.3, Wolfram Research Inc. (1994).
[18] Y. Okamura, M. Torres, E. Blaisten-Barojas, and S. Fujita, Acta Phys. Austriaca **53**, 203 (1981).
[19] Y. Okamura, E. Blaisten-Barojas, S. V. Godoy, S. E. Ulloa, and S. Fujita, J. Chem. Phys. **76**, 601 (1982).
[20] Y. Okamura and H. Miyamoto (unpublished).